Ultra-Large Scale Simulations for Superconductor MgB_2 Device toward Nuclear Application and Fundamental Issues in Nano-structured Superconductors

Project Representative
Masahiko Machida CCSE, Japan Atomic Energy Agency

Authors
Masahiko Machida *1, 5, Takuma Kano *1, 5, Susumu Yamada *1, 5, Toshiyuki Imamura *2, 5, Tomio Koyama *3, 5 and Masaru Kato *4, 5
*1 CCSE, Japan Atomic Energy Agency
*2 University of Electro-Communications
*3 IMR, Tohoku University
*4 Graduate school of Engineer, Osaka Prefecture University
*5 CREST (JST)

This report describes results of the simulation study on the research for superconducting neutron detectors and related fundamental issues on nano-structured superconductors in fiscal year 2007. At first, in order to examine the response speed performance of the superconducting neutron detector using MgB_2, we perform large-scale numerical simulations on non-equilibrium superconducting dynamics after a neutron capture at the superconducting transition edge by solving the time-dependent Ginzburg-Landau equation coupled with the Maxwell and the heat diffusion equations. The large-scale simulations on the Earth Simulator successfully explain the experimental results carried out in JRR-3 (a nuclear reactor in JAEA) and reveal the non-equilibrium superconducting dynamics. In addition, the simulation results suggest a crucial factor in improving the response speed as a neutron detector. On the other hand, as a fundamental research issue of this project, we investigate population imbalance effects in the attractive Hubbard model with confinement potential, which corresponds to spin imbalanced superconductors confined inside nano-scale structures and atomic Fermi gases loaded on an optical lattice. By employing the exact-diagonalization technique as a large-scale numerical tool we reveal that the imbalance and the strong correlation give rise to a specific imbalance structure in charge density profiles, which is observable as atomic density ones in atomic gas systems.

Keywords: Time-dependent Ginzburg-Landau Equation, Non-equilibrium Superconductivity, Neutron Detector, MgB_2, Attractive Hubbard Model, Optical Lattice, Atomic Fermi Gas, Spin Imbalance, Exact Diagonalization

1. Introduction

After the discovery of an alloy superconductor MgB_2 [1], a large amount of experimental studies have been made in order to clarify fundamental aspects of MgB_2. As a result, several novel features including the highest transition temperature among metallic superconductors have been reported, and many ideas toward applications using MgB_2 have been proposed. Among their ideas, an application suggested by Ishida et al. is quite attractive for atomic energy science [2]. The idea is as follows. When a neutron hits on MgB_2 sample, a nuclear reaction occurs between the neutron and an isotope of B, i.e., ^{10}B with a high probability. Then, a fixed nuclear energy is released as an initial kinetic energy of the nuclear reaction products, and the energy transforms into a heat, which leads to an instantaneous destruction of the superconducting state if the temperature is set to be lowered than the superconducting transition temperature. Thus, we can expect that an event of the nuclear reaction is observable as an electrical signal in the superconducting current carrying state [2], since the destruction of superconductivity nucleates a normal spot along which an electrical resistance is generated. This idea is basically equivalent to the detection processes of superconducting Transition Edge Sensor (TES) for X-ray, Superconducting Single Photon Detector (SSPD), and other ones [3]. Thus, a main aim of our project using the Earth Simulator is to simulate the electrical signal generation [4, 5] after the nuclear reaction [6-8] and to provide helpful information to an experimental team making a

neutron detecting device and examining its performance. We believe that the present simulation project enables to avoid wasteful several trial experiments and shorten the development period.

In this fiscal year 2007, our simulation project team made a simulation plan based on experimental results done jointly by Osaka Pref. Univ. and Quantum Beam Science Directorate in JAEA. The experiment was firstly performed on JRR-3 JAEA in 2006 and the first signal for the neutron detection was observed by setting MgB_2 sample under the influence of the neutron irradiation. The time response at the first observation for the single neutron detection is an order of 10 ns, which is completely consistent with our predicted data obtained by this simulation project. Afterwards, the experimental team further advanced the measurement tools and concluded that 1ns is the fastest response time. The speed (1ns) was also proposed in this simulation project. In addition to the speed, the experimental team measured the temperature and the current magnitude dependences of the signal. In the fiscal year 2007, the simulation team aimed at reproducing these dependences and understanding the related non-equilibrium dynamics. A final goal is to answer a question how fast we can tune the detector speed.

All simulations in this fiscal year employed the current biased condition according to the experimental situation. Their results show good agreements with the experimental results. In addition, the results revealed that the local temperature dynamics is much faster than the order parameter and the related electrical field dynamics, which directly affects the signal speed close to the transition. This is because the order parameter relaxation time depends on the ratio of the temperature to the transition temperature and grows toward the transition while the response speed of the local temperature dynamics is not so dependent on the temperature. In other words, this indicates that the local temperature dynamics is irrelevant with the response speed of the electrical signal and the crucial factor to enhance the respond speed is the order parameter relaxation time which abruptly grows close to the superconducting transition. This suggests us how to optimize both the respond speed and the signal intensity.

As another issue of this simulation-based superconducting research, we have done microscopic studies to raise the superconducting transition temperature (T_c) to further high temperature range. Although the issue requires a long time and large resources, it is important for not only fundamental physicist but also engineer since all the superconductor applications now require a large energy cost to cool down the system. Thus, we have started to study the superconductivity mechanism since the fiscal year 2004 [9]. An initial research step for us is to develop numerical schemes to approach the issue. This corresponds to making parallel programs executable on the Earth Simulator, i.e., making efficient parallel codes for the exact diagonalization, the density matrix renormalization group (DMRG) method, Quantum Monte Calro, and so on. We believe that we now have sufficient skills to develop highly parallelized versions for the above former two methods. Actually, in terms of the exact diagonalization, we tested an alternative numerical scheme called "preconditioned conjugate gradient method (PCG)" instead of the traditional Lanczos one, and confirmed that the PCG scheme runs about 5~12 times faster than Lanczos. Moreover, our parallel diagonalization code usually shows the performance exceeding above 50% of the peak on the Earth Simulator. This result is applicable to other wide fields, which need a fast parallelized matrix-diagonalization code. Thus, our tuning results were selected as finalists of Gordon Bell Prize for both 2005 [10] and 2006 [11] years. Generally, since the matrix diagonalization code inevitably requires all-to-all communications which drops the performance, the performance enhancement has never been expected. In this report, we have to avoid describing the details of the tuning due to lack of space, but we would like to just point out that an effective combination of three-level tuning, i.e., the inter-node and the intra-node parallelizations and the vector parallelization, is crucial for effective use of the Earth Simulator.

Our target model for the present quest of superconductivity microscopic mechanism and related topics [12] is the so-called Hubbard model [13]. The model has been regarded as a typical model capturing strongly-correlated behaviors close to the metal-insulator transition. Since the discovery of High-T_c superconductors, the model has been intensively investigated in order to clarify whether or not the model describes high temperature superconductivity exceeding 100K [12]. However, the issue has been not resolved enough yet. This is because it is too difficult to numerically calculate the Hubbard model ($\geqq$2D) in large enough system sizes and to obtain a conclusive result in the thermo-dynamical limit. Especially, the exact diagonalization method has a difficulty that the memory requirement exponentially increases with the number of fermions (electrons) [10, 11] and sites in the model. However, it guarantees the exactness in contrast to other numerical methods which rather require fundamental improvements to obtain reliable results. Namely, the exact diagonalization method enables to touch exact features, if the model system is a finite cluster [10, 11]. This size limitation is not a problem in nano-structured systems and atomic gases, which are intrinsically finite systems. Thus, we studied the Hubbard model with confinement potential [9], which shows features intrinsic to finite systems. For example, it is now known that the confinement potential nucleates the Mott insulator region at the center and the metallic one around the Mott region in the repulsive case. Both of these are essential features of the Hubbard model [9], and the confinement potential

makes it possible to study both of them as a spatially modulated co-existent system [9]. On the other hand, we would like to point out that such a finite system is created in atomic Fermi gases [14] by loading the gas on the optical lattice [15]. This indicates that the numerical result obtained in finite systems can be experimentally confirmed in a direct way.

In this fiscal year 2007, we examined population imbalance effects on the attractive Hubbard model with confinement potential. The main motivation comes from recent experimental developments in atomic Fermi gases, in which various imbalance ratios are easily prepared and the imbalance effects on the confined superfluidity are systematically investigated. In this year, using the parallelized exact-diagonalization code and the density-matrix renormalization group method complementary, we found a specific charge density profile intrinsic to imbalance finite systems. The finding was successfully explained by mapping the Hubbard model into a boson-fermion mixture model including the interaction between the same and the different species.

The contents of this report are as follows. In Section II, the numerical method to simulate the current biased situation is given, and systematic results of large-scale simulations after the neutron capture in MgB_2 are demonstrated. In Section III, the typical density profile structure in the imbalanced attractive Hubbard model with confinement potentials are presented and theoretical analysis on the results are given. See Ref [18] and [19] for more details of results in Section II and III, respectively.

2. Simulations for the Non-equilibrium Superconducting Dynamics after the neutron capture in MgB_2

In this section, we explain the theoretical framework and the numerical simulation method. Subsequently, we give typical simulation results in the current-biased condition. The employed time-dependent Ginzburg-Landau theory has some variations in their validity regimes. Among them, we focus on the most major one, whose valid area is only close to the superconducting transition, i.e., the upper critical field line $H_{c2}(T)$. The time-dependent Ginzburg-Landau equation derived from the theory has a simple damped feature, which is characterized by the relaxation time. Thus, the formalism is very convenient for direct numerical simulation [4]. The time-dependent Ginzburg-Landau equation is given by

$$D^{-1}\left\{\frac{\partial}{\partial t}+i\frac{2e\varphi}{\hbar}\right\}\Delta=-\xi^{-2}\left(|\Delta|^2-1\right)\Delta-\left\{\frac{\nabla}{i}-\frac{2e}{\hbar c}A\right\}^2\Delta=0 \quad (1),$$

where D, φ, and ξ are the normal-state diffusion constant, the scalar potential, and the coherence length, respectively. In Eq.(1), Δ is the normalized complex order parameter and A is the vector potential whose dynamics are described by the Maxwell equation,

$$\nabla\times B=\frac{4\pi}{c}j \quad (2),$$

where the current density j is given by

$$j=\sigma\left\{-\nabla\varphi-\frac{1}{c}\frac{\partial A}{\partial t}\right\}+\mathrm{Re}\left[\Delta^*\left\{\frac{\nabla}{i}-\frac{2e}{\hbar c}A\right\}\Delta\right]\frac{\hbar c^2}{8\pi e}\lambda^{-2} \quad (3),$$

where σ is the normal conductivity, and the first and the second terms stand for the normal and the superconducting current components, respectively. In order to include the local temperature dynamics after the energy release due to the nuclear reaction [6–8], we add the heat diffusion process [5–9] into the superconducting dynamics given by Eq.(1–3). For this purpose, we formulate the energy conservation law which gives a balance between the energy dissipation as Joule heat and the heat flow decomposed into superconducting and normal components given as

$$C_v\frac{dT}{dt}+\frac{dF_s}{dt}+div\left(j_n^Q+j_s^Q\right)+W=0 \quad (4),$$

where C_V, F_s, W and are the heat capacity, the GL free energy, and the Joule heat, respectively, and J_n^Q and J_s^Q are the normal and the superconducting heat currents, respectively. In our simulations, these three equations are coupled and solved together [4–8]. Fifteen years ago, one of the authors (M. Machida) developed a simulation code [4] based on the above formalism without the heat diffusion equation (4) and successfully examined quantized vortex dynamics in the presence of the transport current and applied magnetic field [4]. On the other hand, in the present simulation including Eq.(4), the time development of the temperature is solved as a local variable as well as the order parameter and the vector potential [6–8]. In order to simulate the nuclear reaction inside superconductors, after the fixed heat energy is released on the central top surface of the superconducting strip line, a superconducting region should be destroyed into a normal region, and an electrical voltage should be generated in the current carrying state. By simulating these processes, we can predict how the system responds to the heat generation followed by the nuclear reaction. As a simulation region, the parallelepiped region, which corresponds to a part of a superconducting strip line, is employed and covered by cubic grids as shown in Fig. 1 to discretize Eq.(1–4). The superconducting order parameter and the temperature are given on the grid point, while the vector potential is defined on the link connecting between neighboring grid points as a link variable. This is because the local gauge invariance [4], which is an essential theoretical requirement in charged

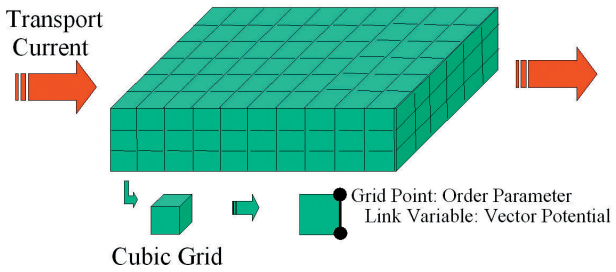

Fig. 1 A schematic figure for the simulation region, which is covered by cubic grids, in which the order parameter (temperature) and the vector potential are defined on the grid point and link, respectively.

superfluidity, should be conserved even in the discrete grid space [4].

The numerical simulation result for the time evolution of the voltage in a typical case, in which T = 38K, T_c = 39K, and the current value is 0.001 of the depairing current at zero temperature, is shown in Fig. 2. From Fig. 2, it is found that the voltage signal is composed of a rapid dip and slow decay structures, which stand for an instantaneous suppression of the superconductivity and a slow relaxation into the superconducting state, respectively. Since the time variation of the local temperature is faster than that of the order parameter, the signal is found to be determined mainly by the relaxation of the order parameter. The typical results are shown below.

Figure 3 shows how the spatial profile of the superconducting order parameter is related to the voltage signal. First, in the minimum of the signal dip as seen in Fig. 3(a), the size of the normal spot is the maximum. Second, the normal spot shrinks together with the signal decay, while the spot region stretches perpendicular to the current direction as seen in Fig. 3(b). Third, only the stretched spot as seen in Fig. 3(c) remains until the recovery to the superconducting state. This stretched behavior becomes more remarkable with increasing the current. On the other hand, the local temperature dynamics are shown in Fig. 4, whose (a) and (b) correspond to the local temperature profile at the same points as Fig. 3(a) and (b), respectively. It is found from these dynamics differences that the temperature dynamics is much faster than the order parameter ones. Since the voltage signal follows the order parameter dynamics, the response time of this type of detector is found to be given by the relaxation time of not the heat but the superconducting order parameter. The reason is simple because the vector potential is directly coupled with the order parameter from Eq.(1–3). This result predicts that the response time is strongly dependent on the operation temperature, i.e., the heat bath temperature. This is because the order parameter relaxation time is dependent on the temperature, i.e., the relaxation time rapidly becomes long when approaching to the superconducting transition. This indicates that if one needs a faster detector then one should decrease the operation temperature as much as possible [18].

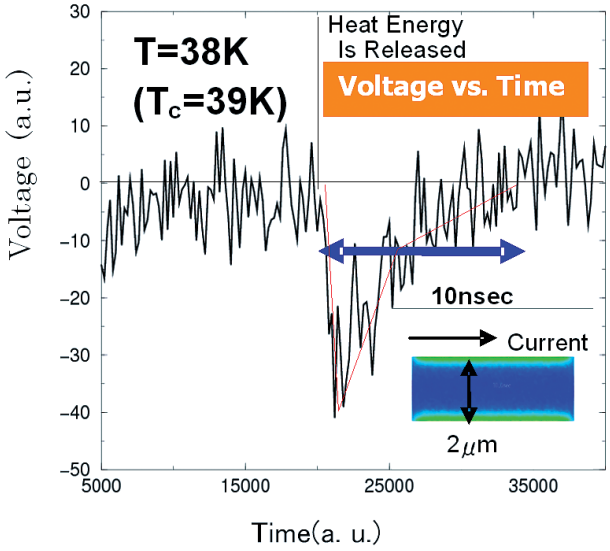

Fig. 2 A simulated time evolution of the measured voltage at 38K (T_c = 39K) for current equal to 0.001j_d(0), where j_d(0) is the de-pairing current at zero temperature. The inset displays an initial profile of the superconducting order parameter in the top surface of the simulation region. The transverse length of the simulated region perpendicular to the current is 2 μm. The red line is a guide for the voltage dip of the signal.

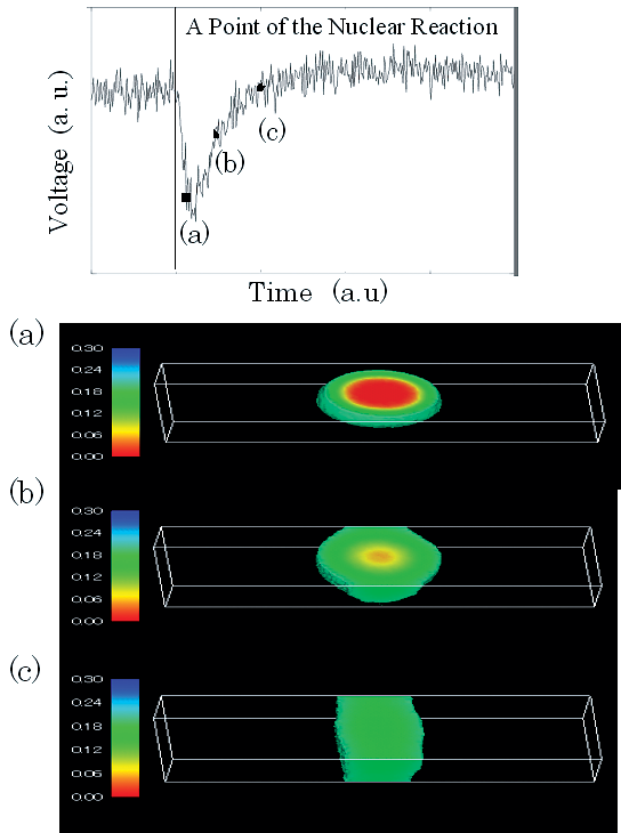

Fig. 3 The voltage signal obtained from the simulation and the spatial profiles of the order parameter at three points (a), (b), and (c) of the signal. The operating temperature is 25K (T_c = 27K), the current density is 0.003j_d(T = 0K), and the current is applied along the long direction.

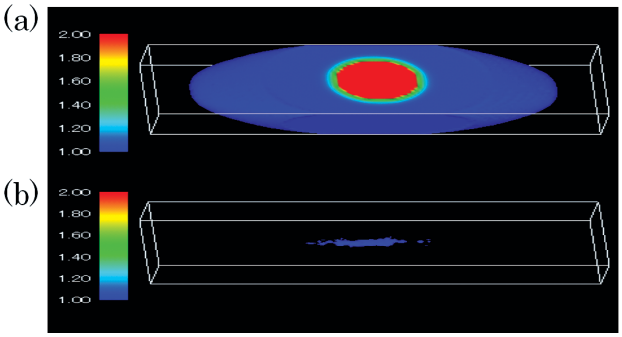

Fig. 4 The spatial profiles of the temperature at two points (a) and (b) of the signal. The other conditions are the same as Fig. 3.

3. Population Imbalance Effects in Attractive Fermion Hubbard Model with Confinement Potential

The Hubbard model [13] is one of the most intensively studied models by computers because it captures very rich varieties of strongly correlated many-body systems although the model expression is quite simple. In the fiscal year 2007, we studied the population imbalance effects on the attractive Hubbard model with confinement potential [9] partly motivated by the rapid advancement of atomic physics [13–14].

Firstly, let us give the Hamiltonian of the Hubbard model with confinement potential as, [9]

$$H = -t \sum_{i,j,\sigma} \left(a^{\dagger}_{j\sigma} a_{j\sigma} + H.C. \right) + U \sum_{i} n_{i\uparrow} n_{i\downarrow} + \left(\frac{2}{N} \right)^2 V \sum_{i,\sigma} n_{i\sigma} \left(i - \frac{2}{N} \right)^2 \quad (5)$$

where t, U, V, and N are the hopping parameter from i-th to j-th sites (normally j is the nearest neighbor site of i), the on-site attractive interaction energy, the parameter characterizing the strength of the trapping potential as schematically shown in Fig. 5, and the site number, respectively. We diagonalized the Hubbard Hamiltonian H (Eq.(5)) [9–11] and calculated the atom density profile. The last term in Eq.(5) describes a harmonic trap potential, in which V gives the potential height at the edge of the lattice. At the edge, the open-boundary condition is imposed. If the atomic density profile sufficiently drops down at the edge, then the boundary condition does not almost affect the result. The parameter V and the total number of Fermi atoms N_F are properly selected to reduce the atom density at the edges. In this report, we examine various population imbalances with keeping $n_{\uparrow}(i) > n_{\downarrow}(i)$ ($N_F = n_{\uparrow}(i) + n_{\downarrow}(i)$). In 1-D cases, we numerically diagonalize the Hamiltonian, Eq.(5) to calculate the density profile at T = 0. Although this approach gives us exact results, the accessible system size is severely limited. To compensate this disadvantage and confirm whether the exact diagonalization results are small size effects or not, we employ the Density-Matrix Renormalization Group Method (DMRG). The DMRG guarantees a high accurate result as long as the

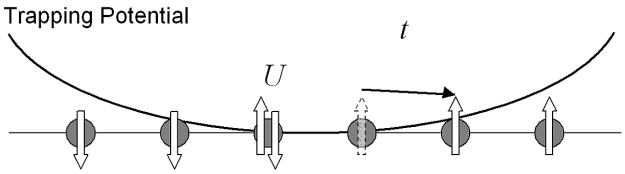

Fig. 5 A schematic figure for the fermion-Hubbard model with confinement potential.

trap potential is not so steep. On the other hand, in two-dimensional (2-D) square lattice systems, we use solely the exact diagonalization, because the method is now the most accurate and reliable for 2-D finite systems. We are now developing an accurate DMRG method on 2-D systems by parallelizing DMRG code. For the exact diagnolization and the DMRG, we use SX-6 (1-node 4CPU's system) and Altix 3700Bx2 in JAEA and the Earth Simulator, respectively. In the exact diagonalization, the problems with the lattice size N = 16 are calculated by SX-6, while those with above N = 20 the Earth Simulator. In 2-D case, we set N = 25, which requires 128 nodes (1024CPU's) on the Earth Simulator. In the case, we need parallelization and high-performance computing techniques. See Ref.[10, 11] for computational technical issues on massively parallel supercomputers.

Let us present exact diagonalization results for the imbalanced 1-D Hubbard model with the trap potential. Figure 6 shows U/t dependence of the calculated atom-density profile of the ground state, $n(i) = n_{\uparrow}(i) + n_{\downarrow}(i)$, for three population imbalances, whose ratios of major to minor species are (a)5:3, (b)6:2, and (c)7:1, respectively. For these three cases, the lattice size N = 16, the total number of fermions $N_F = 8$, and V/t = 1. The filling is just the quarter one if the trap potential does not exist. Although the depression at the edges is not completely zero in the presence of the trap V/t = 1, we confirm that there are no edge effects because of no significant change of profiles on the lattice size extension (N = 18 and 20) with the same fermion number (see Fig. 6(d)). In each panel of Fig. 6, we find a step-like structure (see arrow in each figure) in each dome like profile. This structure becomes more pronounced as one increases the amplitude strength of the attractive interaction |U|. The structure is also observable in Fig. 6(d) with a larger size (N = 20), in which N_F and V/t is the same as (a–c), and U/t is fixed to be –10.

The step-like structures seen in Fig. 6 are found to be associated with the phase separation between a core phase whose main component is pair and a shell one composed of only unpaired excess atoms from other observables as shown in Fig. 7. Figure 7 (a), (b), (c) and (d), respectively, show U/t dependent profiles of the single-occupation density $n_F(i)$, the double-occupation density $n_B(i)$, the density subtraction $n_{\uparrow}(i) - n_{\downarrow}(i)$, and the on-site pair amplitude Δ(i) (see Ref. [9] for the definition). $n_F(i)$ and $n_B(i)$ are calculated by picking up the

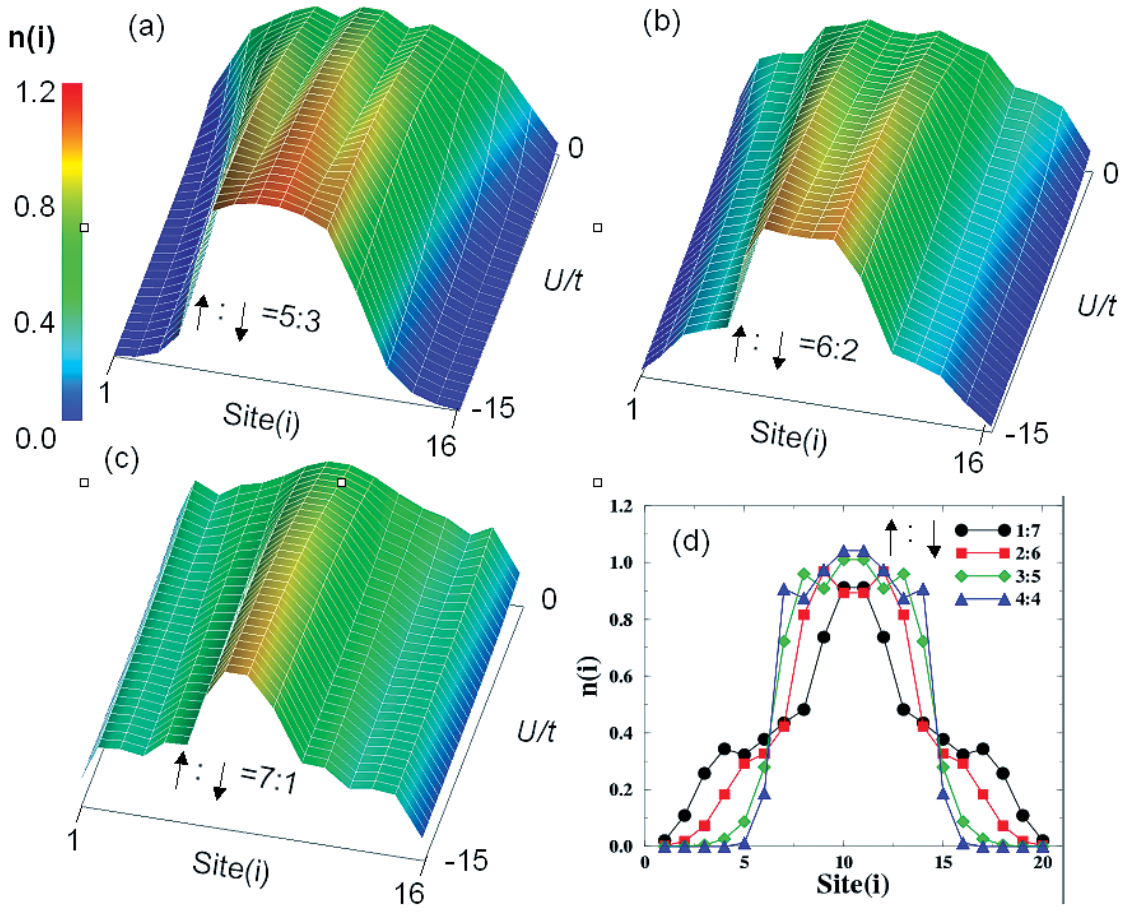

Fig. 6 The exact diagonalization results for U/t dependences ($-15 \le U/t \le 0$) of particle density profiles, n(i) for three imbalance cases, whose ratios of major to minor fermion species are (a) 5:3, (b) 6:2, and (c) 7:1, respectively. In these three cases, $N_F = 8$, $N = 16$ and $V/t = 1$. The panel (d) is a highlight of n(i) at $U/t = -10$ for the imbalance from 4:4 to 7:1 in $N = 20$. N_F and V/t are the same as (a–c).

coefficient of the eigen-state whose i-th site occupation is 1 and 2, respectively, from the ground state wave-function and summing up the amplitude of the coefficient. For the methodological details to calculate them, see Ref.[20]. According to Ref.[20], as |U/t| increases in the balanced case, $n_F(i)$ decreases, while $n_B(i)$ instead increases. This simple relationship means that the Cooper pair becomes more tightly-bounded one on a site with increasing |U/t|. From Fig. 7, we clearly find that $n_B(i)$ and $\Delta(i)$ well develop only inside the "phase boundary" characterized by the step-like structure as seen in Fig. 6 while they completely diminish outside the boundary (shell region). This tendency becomes more pronounced with increasing the attractive interaction and saturated in the strong limit. This suggests that the pair density and the superfluid order locally develop inside the core. This does not contradict a consensus that the superfluid correlation grows as the most dominant one in 1-D attractive Hubbard model. Thus, we call the core region "superfluid core" in the following. However, we note that there is a subtle issue whether the core really exhibits superfluidity or not due to its dimensionality and finiteness. The discussion originates from a problem how stable the superfluid ground state is against fluctuations. This is beyond information obtained by the present methods (the exact diagonalization and DMRG), which mainly solves the ground state. Thus, we do not discuss stability of the superfluidity but concentrate on its charge density profile in this report. Fig. 7(a) reveals that un-paired component stays even in the core region, where the $n_B(i)$ and $\Delta(i)$ grow. As a result, the density difference $\delta n(i) = n_\uparrow(i) - n_\downarrow(i)$ does not vanish in the core region as seen in Fig. 7(c).

Generally, we find that $n_\uparrow(i) : n_\downarrow(i) \sim 2{:}1$ in the core region except for a very weak coupling regime (compare Fig. 6(b) with Fig. 7(c)). This result is in contrast to the experimental observation in atomic gases without the optical lattice, in which the phase separation between Cooper-pair superfluid phase and normal polarized one occurs. We would like to point out that the present result can be well explained by an effective theoretical model for the imbalanced attractive Hubbard model. The effective model is a boson-fermion mixture model which includes a boson-fermion interaction in addition to the boson-boson and the fermion-fermion interactions. In this effective model, the boson-fermion interaction intrinsic to the lattice system gives rise to a big difference between non lattice and lattice systems.

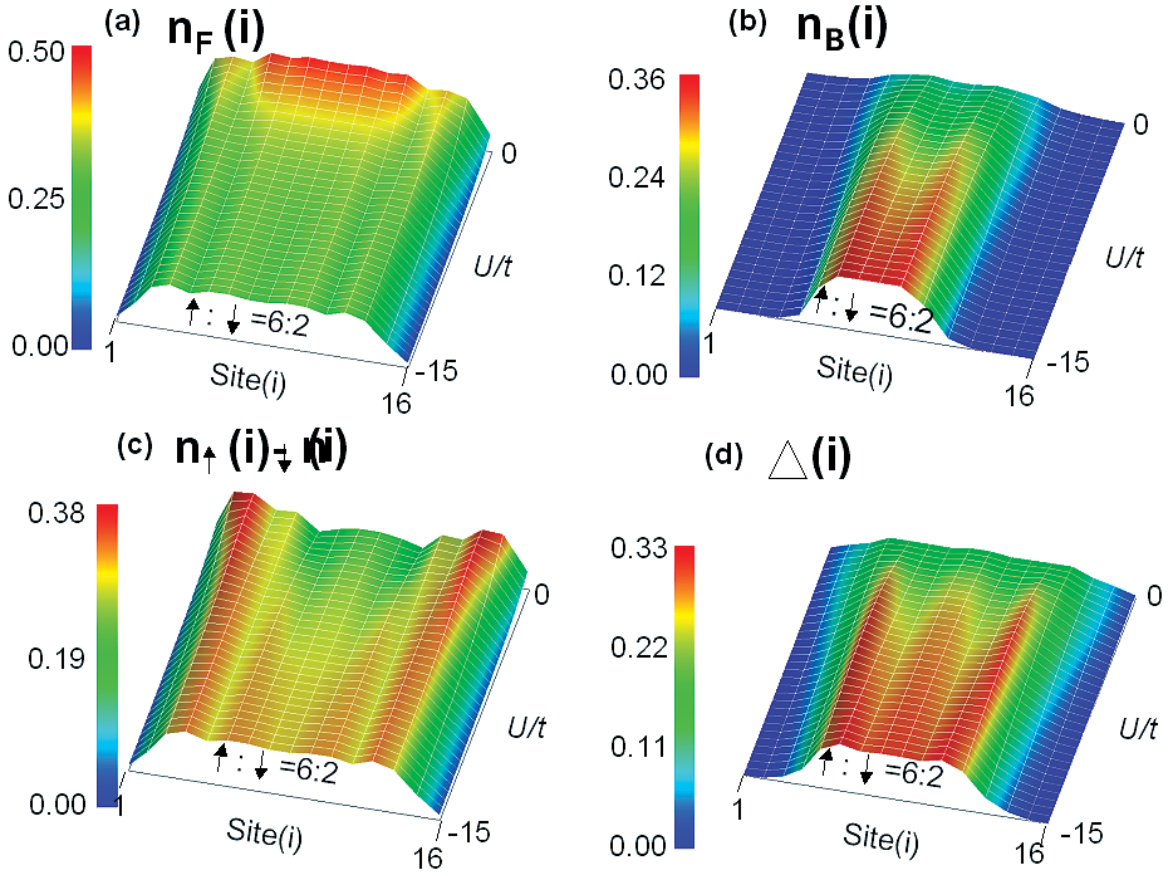

Fig. 7 The exact diagonalization results for U/t dependences (–15 ≤ U/t ≤ 0) of profiles of (a) the single occupation density $n_F(i)$, (b) the double occupation density $n_B(i)$, (c) the subtraction from major to minor species density $n_\uparrow(i) - n_\downarrow(i)$, and (d) the on-site pair amplitude Δ(i). In all the cases, NF = 8 (6↑, 2↓), and other conditions are the same as those of Fig. 6 (a–c).

4. Summary and Conclusion

We numerically studied two kinds of topics related to superconductivity. The main result in terms of the first topic was that the signal speed strongly depends on the heat bath temperature. We successfully finished test simulations and actually confirmed the temperature dependence. For the second topic, we calculated the charge density profiles in order to clarify the population imbalance effects on the confinement situation, which was modeled by the attractive Hubbard model with the confinement potential.

References

[1] J. Nagamatsu, N. Nakagawa, T. Muranaka, Y. Zenitani, and J. Akimitsu, Nature **410**, 63(2001).

[2] K. Takahashi, K. Satoh, T. Yotsuya, S. Okayasu, K. Hojou, M. Katagiri, A. Saito, A. Kawakami, H. Shimakage, Z. Wang, and T. Ishida, Physica C **392–396**, 1501(2003).

[3] See, e.g., D. Fukuda, H. Takahashi, M. Ohno, and M. Nakazawa, Nucl. Instr. and Meth., A**444**, 241(2000).

[4] M. Machida and H. Kaburaki, Phys.Rev.Lett.75, 3178(1995); M. Machida, A. Tanaka, and M. Tachiki, Physica C**288**, 199(1997).

[5] I. Shapiro, E. Pechenik, and B. Ya. Shapiro, Phys. Rev. B **63**, 184520 (2001).

[6] M. Machida, T. Koyama, M. Kato, and T. Ishida, Nucl. Instr. and Meth., A**529**, 409(2004).

[7] M. Machida, T. Koyama, M. Kato, and T. Ishida,, Physica C**426–431**, 169(2005).

[8] M. Machida, T. Koyama, M. Kato, and T. Ishida, Nucl. Instr. and Meth..A**559**, 594(2006).

[9] M. Machida, S. Yamada, Y. Ohashi, and H. Matsumoto, Phy. Rev. Lett. **93**, 200402(2004).

[10] S. Yamada, T. Imamura, and M. Machida, Proc. of SC2005, (2005). http://sc05.supercomputing.org/schedule/pdf/pap188.pdf.

[11] S. Yamada, T. Imamura, T. Kano, and M. Machida, Proc. of SC2006, (2006). http://sc06.supercomputing.org/schedule/pdf/gb113.pdf.

[12] See, e.g., M. Tachiki, M. Machida, and T. Egami, Phys. Rev. B**67**, 174506(2003).

[13] See, e.g., *The Hubbard Model, Recent Results*, ed. M. Rasetti (World Scientific, Singapore, 1991); *The Hubbard Model*, ed. A. Montorsi (World Scientific, Sigapore,

1992).

[14] C. A. Regal, M. Greiner and D. S. Jin, Phys. Rev. Lett. **92**, 040403 (2004).

[15] M. Greiner, O. Mandel, T. Esslinger, T. W. Hansch, and I. Bloch, Nature **415**, 39(2002).

[16] M. Machida and H. Kaburaki, Phys.Rev.Lett., 71, 3206(1993).

[17] M. Machida, S. Yamada, Y. Ohashi, H. Matsumoto, Phys. Rev. Lett., **95**, 218902(2006).

[18] M. Machida, T. Kano, T. Koyama, M. Kato, and T. Ishida, J. Low Temp. Phys.**151**, 58(2004).

[19] M. Machida, S. Yamada, M. Okumura, Y. Ohashi,, H. Matsumoto, Phys. Rev. A (in press).

[20] M. Machida, S. Yamada, M. Okumura, Y. Ohashi,, H. Matsumoto, Phys. Rev. A74(2006)053621.

MgB_2超伝導体における中性子捕獲後の非平衡ダイナミクスと原子気体ハバードモデルでのスピン偏局効果

プロジェクト責任者
町田　昌彦　　日本原子力研究開発機構　システム計算センター

著者
町田　昌彦*1,5，叶野　琢磨*1，山田　　進*1，今村　俊幸*2，小山　富男*3,5，加藤　　勝*4,5
*1　日本原子力研究開発機構　システム計算センター
*2　電気通信大学
*3　東北大学　金属材料研究所
*4　大阪府立大学　工学研究科
*5　CREST（科学技術振興機構）

1. プロジェクトの概要

最近発達してきた超伝導ナノファブリケーションのテクニックにより全く新しいタイプの超伝導デバイス開発の可能性が開けてきた。これを受けて本プロジェクトでは、以下の3つの新しい超伝導デバイス開発に関連したシミュレーション研究を行う。

1）中性子飛来の時系列を検出する高速応答超伝導デバイス開発先導のためのシミュレーション研究。
2）1）のテーマを基礎からサポートし、かつ、新しいナノスケールでの新奇超伝導物理現象を探索するための研究。
3）高温超伝導体と金属超伝導体とをモザイク状に配置するなど、ナノ量子ドットデバイスのシミュレーション研究。

テーマ1）では、コンソーシアムの複数の実験グループと協力し、高精度中性子検出デバイス開発を先導するためのシミュレーション研究を行う。テーマ2）では、ナノスケールでの超伝導発現機構やその微視的状態を明らかにするため、ナノ超伝導体やそれと同等なフェルミ原子ガスの基底状態の探索を行う。 テーマ3）では、量子コンピュータ・キュビット素子モデルの一つとして其の将来性が評価されている超伝導体界面に現れる縮退半磁束のダイナミクス等、斬新なアイデアに基づく超伝導デバイス応用を指向した大規模シミュレーション研究を行う。

2. 得られた成果(2007年度)の概要

今年度得られた成果の一つは、①上記テーマ1）の超伝導体MgB_2の中性子捕獲後の超伝導非平衡ダイナミクスのシミュレーションを超伝導転移点近傍という実験条件とほぼ同等の条件下で行い、実験観察結果の再現（中性子検知シグナルの電流依存性や温度依存性等）に成功したことである。また、超伝導特有の超高速応答をどのような原理に基づき実現できるかを明らかにできたことである。もう一つの成果は②上記テーマ2）に関連してナノスケールに閉じ込められた強相関電子系（理論的に同等な系としてフェルミ原子ガス）のスピン偏局効果を系統的に計算し、偏局度合等によらずにほぼ普遍的な粒子密度分布を示すことを明らかにしたことである。以下に具体的な成果の概要を記す。

1）超伝導体MgB_2に中性子が照射されるとB（ボロン）の同位体^{10}Bは核反応を起こし、一定の運動エネルギーを持ったα粒子が射出される。この際、荷電粒子であるα粒子は物質内で原子と衝突を繰り返し、そのエネルギーは熱へと変換され、超伝導の破壊に到り、電気信号として観察される。本年度はこの電気信号の電流依存性や温度依存性等、実際に観察された結果を再現し、更に、それらの依存性を与えるメカニズムを研究した[1]。その結果、応答速度を上昇させるための指針を得ることができた。
2）一般に酸化物高温超伝導体に代表されるような電子相関の極めて強い系の代表的理論的モデルとしてハバードモデルがあるが、当プロジェクトではこのハバードモデルに対し、調和ポテンシャルを付加し、フェルミオン粒子（電子）を中心部に閉じ込める派生モデル（固体の場合は、ナノスケールに強く閉じ込められた電子系に相当する一方、フェルミ原子ガスの場合は、現在、実験が用いている条件と合致する）に着目し、その大規模ハミルトニアン行列（最大で千数百億次元に達する）の数値対角化を行っている。本年度は、このモデルに対し、スピンの異なる粒子数のバランスが壊れ、スピン偏局がある場合の量子状態についての計算を行った。その結果、スピン偏局がある場合、粒子分布に特有の構造（中心部の偏局度はほぼ一定となる）が現れることを見出した。詳細については[2]を参照されたい。

＜代表的出版論文＞

[1] M. Machida, T. Kano, T. Koyama, M. Kato, and T. Ishida, "Direct Numerical Simulations for Non-equilibrium Superconducting Dynamics at Transition Edge: Simulation for MgB_2 Detectors", J. Low Temp. Phys., A559,

594(2005).
[2] M. Machida, S. Yamada, M. Okumura, Y. Ohashi, and H. Matsumoto, "Correlation effects on atom-density profiles of one- and two-dimensional polarized atomic Fermi gases loaded on an optical lattice", Phy. Rev. A(in press).

キーワード：ナノ超伝導体, 非平衡超伝導, 中性子検出, 超伝導発現機構, MgB_2